Asian Journal of Chemistry; Vol. 35, No. 9 (2023), 2265-2274

ASIAN JOURNAL OF CHEMISTRY

https://doi.org/10.14233/ajchem.2023.28243

Electronic Spectroscopy and Molecular Modelling Study of Supramolecular Receptors based on Azo Compound of *o*-Toluidine Capable of Sensing Mercuric Ion

RIDIP DAS, RAJIB LOCHAN SARMA and DIPJYOTI KALITA*

Department of Chemistry, Bhattadev University, Bajali-781325, India

*Corresponding author: E-mail: che.dipjyoti@bhattadevuniversity.ac.in

Received: 28 June 2023; *Accepted*: 10 August 2023; *Published online*: 31 August 2023; AJC-21374

Two supramolecular receptors capable of binding anion as well as metal ion were synthesized by linking *o*-toluidine with 2,6-diaminopyridine and 4-aminopyridine *via* diazocoupling reaction. The interaction of the receptors with different acids and metal ions were studied in solution state by using UV-visible titration. One of the receptors is capable of sensing Hg^{2+} ion in solution state by showing considerable amount of bathochromic shift in its absorption maxima. Their binding affinities were also compared by calculating binding constants from the UV-visible titration data. A theoretical study was carried simultaneously to investigate the plausible interaction of host-guest complexes. The different binding affinities were calculated from the free energy change data and compared with the experimental values. The possible structure of metal complexes of Hg^{2+}, Cu^{2+} and Fe^{2+} ions were optimized and their properties were also studied. The limit of detection (LoD) of Hg^{2+} ions was found to be 0.223 ppm.

Keywords: Isosbestic point, Bathochromic shift, Binding constant, Mulliken charge density.

INTRODUCTION

The role of anions in the field of medicine [1-3], material science [4-6], electrochemistry [7,8] *etc*. are undeniably of prime importance in modern day research. Many important biomolecules are present in human body in their anionic form which works through electrostatic force in addition to other weak interactions. Owing to their vast utility in the biological system, the study of the behaviour of anions with other molecules becomes essential. Further the role of metal ions in every field of science is well established which prompts the researchers to observe and analyze the effect of metal ions in every possible way [9-11]. The application of azo compounds in the field of the printing and textile industries are well-known [12,13]. In addition, these compounds find applications in almost every field of science such as indicators, cosmetics, food colouring, plastics, optical switch, optical data storage, nonlinear optics, liquid crystal displays and electro-optical devices *etc*. [14,15]. Biological activity of aryl diazonium compounds and diazonium salts are also well established [16,17].

Many azo compounds are reported to be sensors for important anions such as fluorides, phosphates, biphosphates, acetate, cyanide, *etc.* [18-21]. Azo compounds based on heterocycle is used for colorimetric determination of cyanide ions in solutions [22]. Ligands based on azo compounds have been synthesized and the structure of their metal complexes are also reported [23]. Transition metal complexes of azo compounds are found to show antimicrobial activities [24]. Interesting spectroscopic properties of azo-dyes and azo-metal complexes are also known [25]. Many diazo compounds are reported to be used as photosensitizers [26]. Supramolecular receptors of azo dyes and their metal complexes are prepared and the weak interactions were studied from their crystal structures [27]. Further, the interactions of these azo compounds with different guest molecules are also established by molecular modeling and DFT calculations [28,29]. The diazo coupling reactions of toluidine was reported way back in 1936, however the anion and metal binding properties of such compounds are yet to be explored [30].

Inspiring from these enormous scope of applications, we have synthesized two *o*-toluidine based azo compounds (**L1** and **L2**) having a heterocyclic moiety attached and studied their anion and metal binding properties.

EXPERIMENTAL

All the chemicals and solvents were of highest analytical grade quality and procured from various commercial sources. The UV-visible spectra were recorded on a Perkin-Elmer LAMBDA 365 UV/Vis spectrophotometer. IR-spectra were recorded on SHIMADZU IR Spirit Fourier transform infrared spectrophotometer. Mass spectra recorded on a Waters Xevo G2-XS QT of high-resolution mass spectrometer. All the data were recorded at room temperature.

The synthesis of both supramolecular receptors (**L1** and **L2**) based on azo compounds were done according to the reported method [31].

Synthesis of 3-(*o*-tolyldiazenyl)pyridine-2,6-diamine (L1): *o*-Toluidine (0.212 g, 1 mmol) dissolved in dil. HCl was added to 1.4 g of sodium nitrite solution with constant stirring. A solution of 2,6-diaminopyridine (1 mmol; 0.901g) in 10 mL of 2.5 M NaOH was added into the above solution kept in an ice bath. The reaction mixture was stirred at room temperature for 30 min, which gives a red coloured product (**Scheme-I**). The crude product was recrystallized from ethanol. Yield: 72%; m.p.: 280 ºC; HRMS, *m/e* (relative intensity) 227 (M+1); IR (KBr, cm^{-1}): 3459 (bs), 1637 (m), 1618 (s); λ_{max} (methanol) = 381 nm (ε = 815.1 mol^{-1} cm^{-1}).

Synthesis of 3-(*o*-tolyldiazenyl)pyridin-4-amine (L2): *o*-Toluidine (0.212 g, 1 mmol) dissolved in dil. HCl was added to 1.4 g of sodium nitrite solution with constant stirring followed by the addition of 4-aminopyridine (1 mmol; 0.0941 g) in 10 mL of 2.5 M NaOH was added into the above solution kept in an ice bath. The reaction mixture was stirred at room temperature for 30 min, which gives a red coloured product (**Scheme-I**). The crude product was recrystallized from ethanol. Yield: 76%; m.p.: 280 ºC. HRMS, *m/e* (relative intensity) 212 (M+1); IR (KBr, cm^{-1}): 3470 (bs), 1647 (m), 1627 (s); λ_{max} (methanol) = 377 nm (ε = 614.9 mol^{-1} cm^{-1}).

Procedure of UV-visible titration: Methanolic solution (1×10^{-4} M) of synthesized two azo linked supramolecular receptors (**L1** and **L2**) were taken in a cuvette and a constant aliquot of (50 µL) of the guest acids and metal salts solutions (1×10^{-4} M) were added. In all cases, chloride salts of the respective metal ions were used (except for Fe^{2+} ions, the sulphate salt was used).

Limit of detection (LoD) calculation: The limit of detection (LoD) is determined as 3(σ/K), where σ and K represent the calculated standard deviation of intercepts and the slope of the absorption calibration curve, respectively. The standard deviation was calculated from the standard error and the sample size by the relation SE = SD/√(sample size) [32].

Methodology of theoretical investigation: Theoretical investigation has been performed in G16 program series [33] by employing DFT calculation in gas phase. Hybrid density functional, M06-2x has already proved its notable performance in the study of the non-covalent interaction in comparison to the commonly used DFT calculation [34]. In current study, therefore, M06-2x functional was considered and the basis set def2svp is used for geometry optimization and frequency calculation.

RESULTS AND DISCUSSION

Two azo linked supramolecular receptors (**L1** and **L2**) were prepared by reaction of *o*-toluidine with a mixture of dil. HCl and $NaNO_2$ by keeping the reaction mixture at below 5 ºC, followed by reaction with an alkaline solution of 2,6-diaminopyridine and 4-aminopyridine, respectively (**Scheme-I**) and they were further characterized by melting point, FT-IR, UV-visible spectroscopy and LCMS.

Interaction of anions with L1 and L2 in solution state: The anion recognition properties of both compounds were studied in solution state by using UV-visible spectrophotometer. Solutions of known concentration in methanol of the compounds were titrated against the respective acids of the corresponding anions. As the host molecules (**L1** and **L2**) contain basic nitrogen atoms, it is expected that the guest acids will protonate the corresponding hosts thereby modifying the host's electrostatic property. Hence, in this case, the protonated form of **L1** and **L2** actually acts as host for the anion and a 1:1 host-guest binding may be expected as depicted in Fig. 1.

The UV-visible titrations of **L1** and **L2** with different acids show its diverse affinity towards the acids and the correspon-

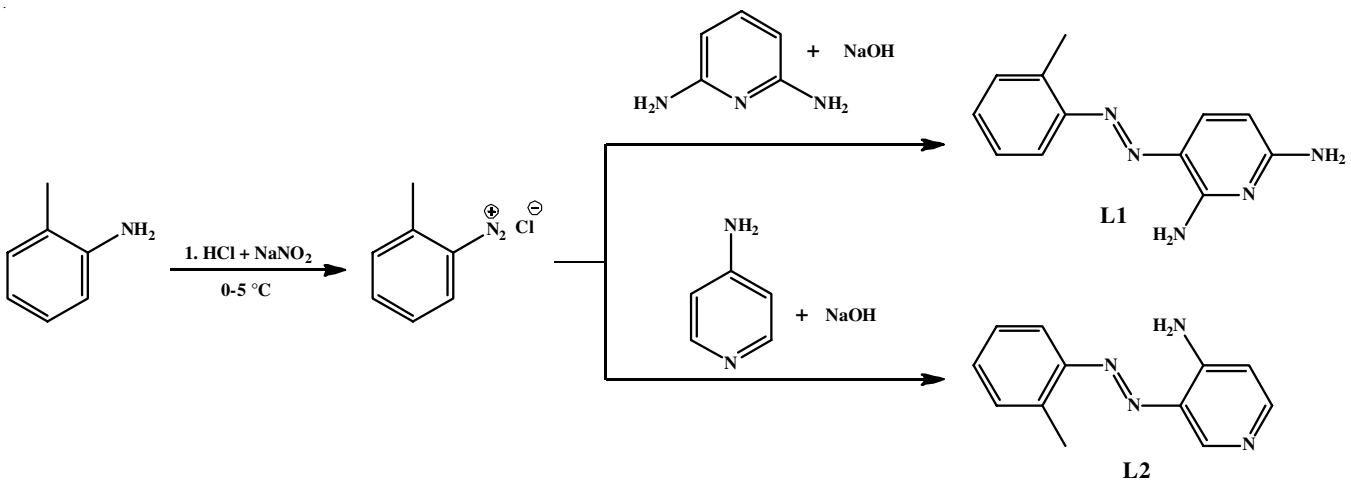

Scheme-I: Synthetic route to the receptors **L1** and **L2**

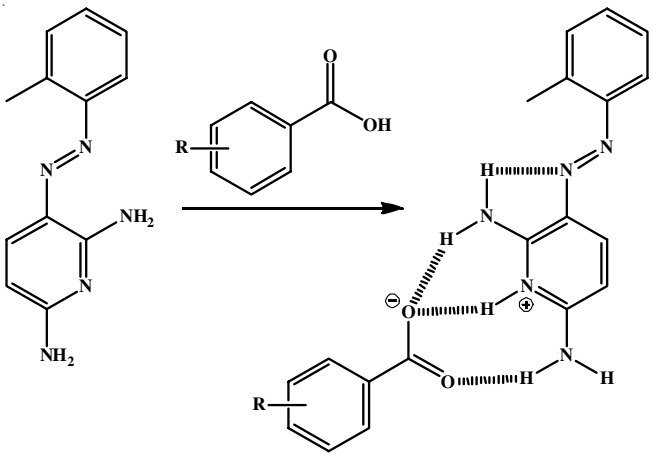

Fig. 1. A predicted 1:1 binding model of protonated **L1** and anion

ding anions. A representative case of comparison of interactions of **L1** and **L2** with various acids is shown in Fig. 2a-b, respectively. The azo compounds are known for their characteristic low energy n to π* transition [35,36]. The host **L1** forms an absorption maximum at 381 nm corresponding to an n to π* transition with a molar extinction coefficient of 815.1 L mol^{-1} cm^{-1}. The peak gradually decreases on addition of guest acids with a simultaneous increase of absorption at 301 nm thereby forming an isosbestic point. The new peak is attributed to the protonated form of **L1** which gradually increases on increasing concentration of the corresponding acids. The n to π* transition peak generally shifts to lower wavelength (higher energy) region of the electromagnetic spectrum in case of a positively charged species; as the positive charge will make the transition more difficult and hence higher energy will be required for the transition. However, a similar phenomenon is not observed in case of all the guest acids, which clearly depicts the ability of the receptors to distinguish between the guest acids.

Salicylic acid, cinnamic acid and oxalic acid are capable of protonating **L1** to a significant amount and show a similar titration curve with clear isosbestic point (Fig. 3a). Isosbestic point indicates the equilibrium of **L1** with its protonated form. Whereas, benzoic acid and succinic acid are unable to protonate **L1** and shows a completely different type of titration curve (Fig. 3b). In order to confirm the protonation phenomena **L1** was titrated with relatively strong mineral acids such as sulphuric acid, nitric acid and hydrochloric acid, which also show isosbestic point and a new peak at 301 nm.

On the other hand, receptor **L2** shows absorption maxima at 377 nm with a molar extinction coefficient of 614.9 L mol^{-1} cm^{-1}. The peak at 377 nm shows a gradual decrease on addition of salicylic acid and cinnamic acid with a simultaneous increase of absorption maxima at 298 nm (Fig. 3c). An appearance of new peak at 298 nm is not observed in case of succinic acid. So far these observations are similar to that of **L1**, which shows the ability of guest acids to protonate the host receptor **L2** with an exception of benzoic acid (Fig. 3d) which is able of protonate **L2** but not **L1**.

Unlike **L1**, receptor **L2** shows bathochromic shift in its absorption maxima with some guest acids. On interaction of oxalic acid, the original peak at 377 nm gets shifted to 384 nm, with nitric acid and hydrochloric acid the peak is further shifted to 385 and 387 nm, respectively (Fig. 4). This significant red shift in absorption maxima is not only due to simple protonation of the receptor molecule but may be attributed to additional interaction of the corresponding anion with the receptor **L2** in solution state.

The binding affinity of all the guest molecules with both **L1** and **L2** were studied by calculating their respective binding constants from UV-visible titration data by using the following equation:

$$\frac{L}{\Delta\varepsilon_{ap}} = \frac{L}{\Delta\varepsilon} + \frac{1}{\Delta\varepsilon \times K}$$

where L is the concentration of host molecule in molarity; $\Delta\varepsilon_{ap} = |\varepsilon_a - \varepsilon_f|$ and $\Delta\varepsilon = |\varepsilon_b - \varepsilon_f|$, where, ε_b and ε_f are respective extinction coefficients of the host compound in the presence and absence of guest molecules. The apparent extinction coefficient (ε_{ap}) was obtained by calculating A_{obs}/[host] where A_{obs} was the observed absorbance. The data were fitted to the above equation to obtain a straight line with a slope = 1/ε and y-intercept = 1/(ε×K). The binding constants K were deter-

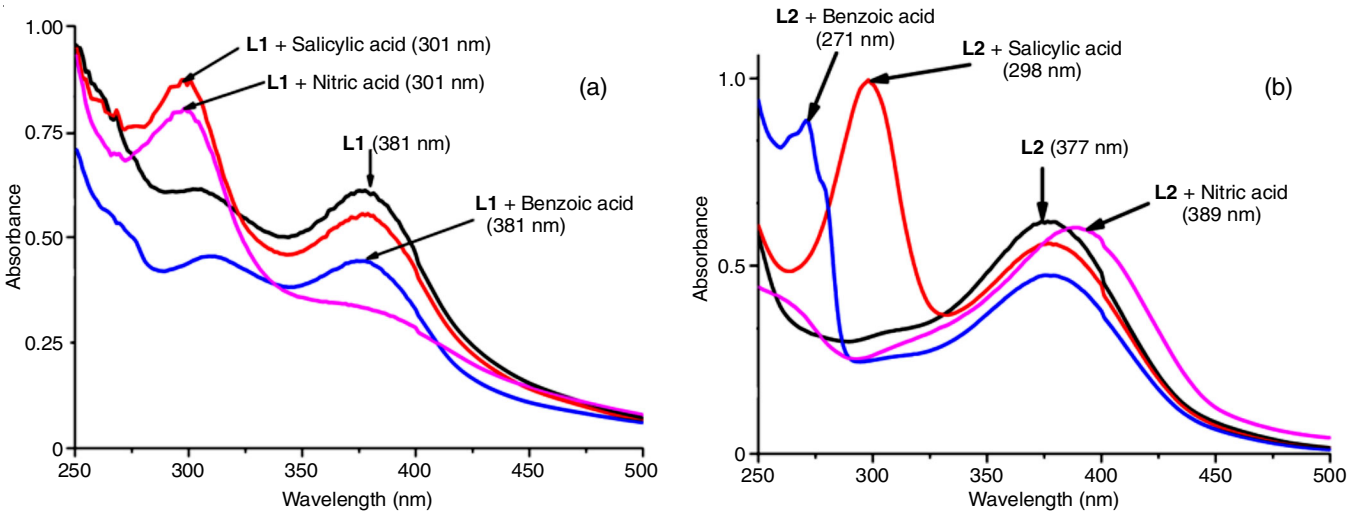

Fig. 2. Comparison of UV-visible spectra of **L1** and **L1** + Guest acids (a) and **L2** and **L2** + Guest acids (b)

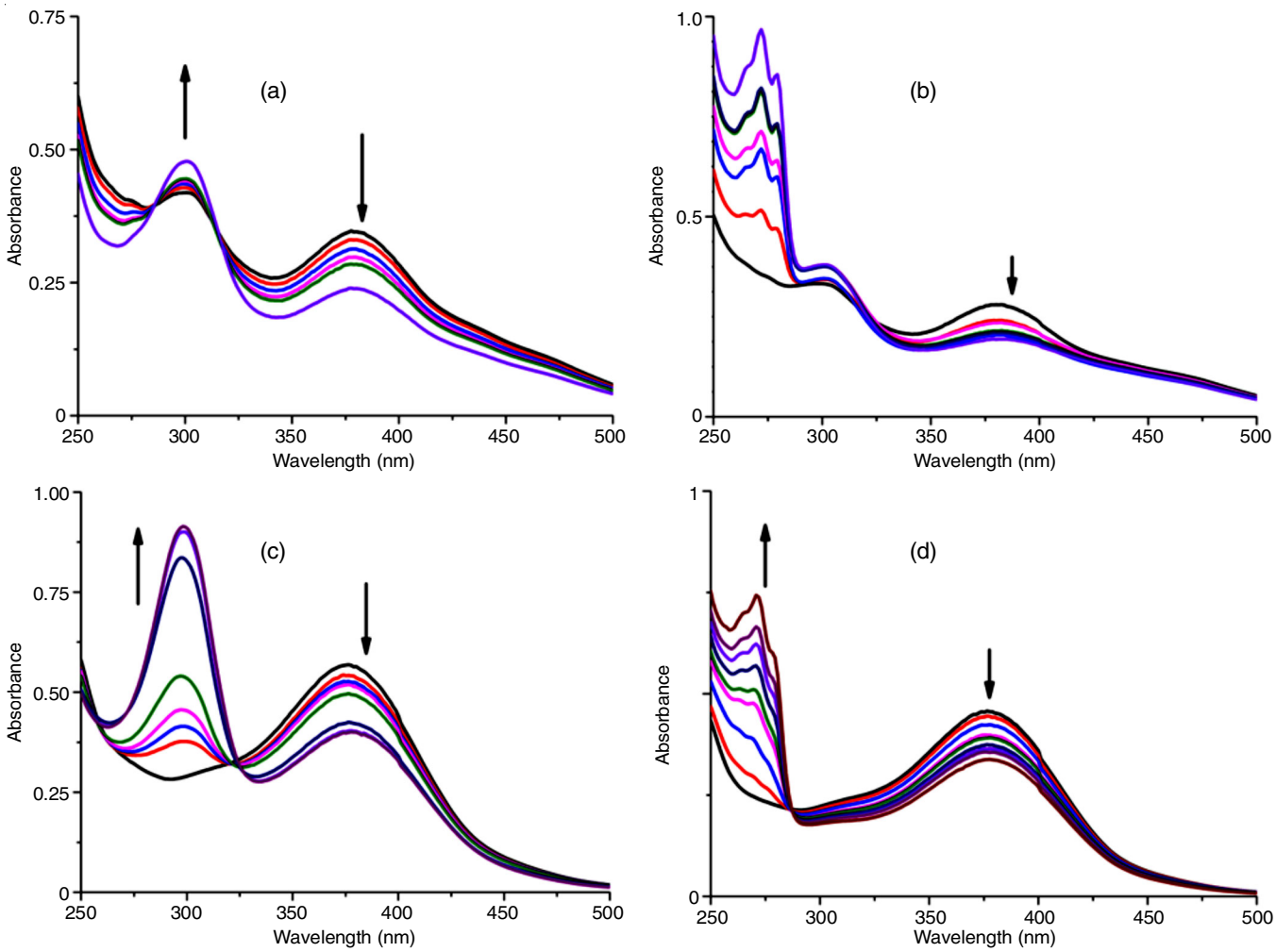

Fig. 3. UV-visible titration of **L1** and **L2** in the presence of increasing amounts of salicylic acid (a,c = **L1** and **L2**, respectively) and benzoic acid (b,d = **L1** and **L2**, respectively)

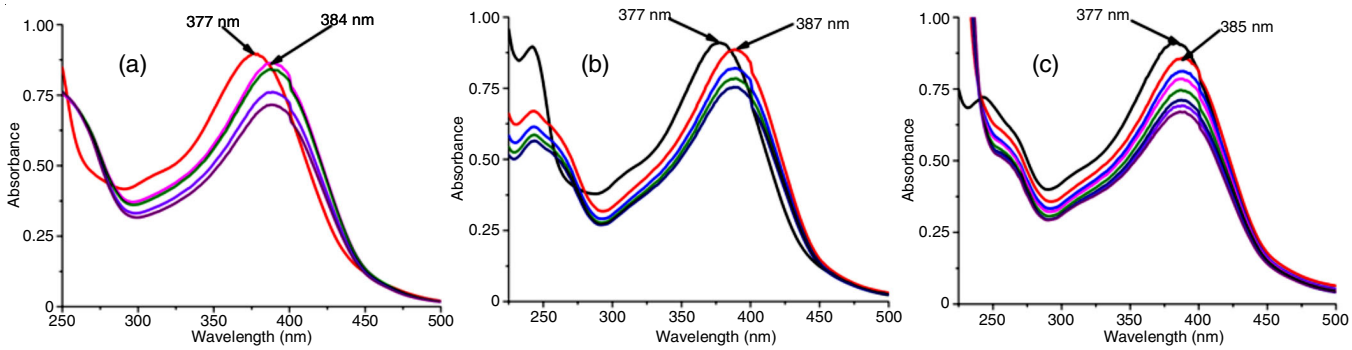

Fig. 4. UV-visible titration of receptor**L2** ([**L2**] = 1×10^{-4} M in Methanol) in the presence of increasing amounts of oxalic acid (a), hydrochloric acid (b) and nitric acid (c)

mined from the ratio of the slope to the y-intercept [37]. For each host-guest couple the experiment was repeated three times to obtain the best fit curve as represented in Fig. 5a-b.

A brief comparison of binding constants of **L1** and **L2** are illustrated in Fig. 6a-b, respectively. From this comparison data, it is visible that the host **L1** shows highest affinity towards salicylic acid and benzoic acid although the titration curves for both acids are not similar (Fig. 3a-b). Benzoic acid did not show the formation of isosbestic point with **L1** whereas salicylic acid forms two clear isosbestic points. This observation prompted to predict that benzoic acid is not able to protonate **L1** but it is capable to interact by virtue of other weak interactions in solution state.

However, in case of **L2** benzoic acid shows comparatively less binding affinity (Fig. 6b), which may be attributed to the presence of less number of hydrogen bonding site in **L2** as compared to **L1**. The other acids such as sulphuric acid, nitric acid, hydrochloric acid, oxalic acid, salicylic acid show good

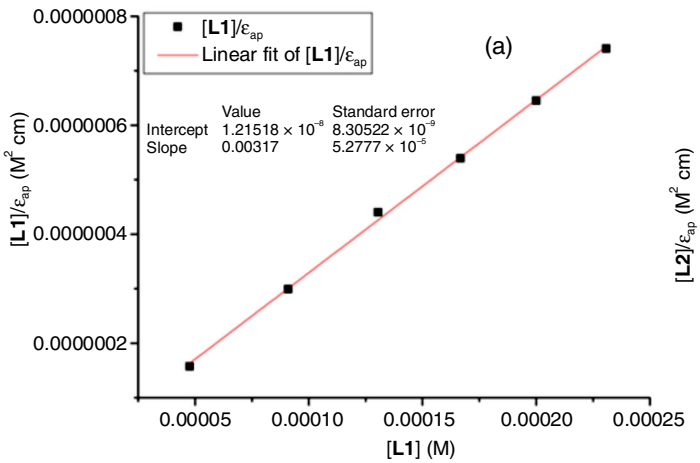

Fig. 5a. **L1**–Salicylic acid: plot of [**L1**]/ε_{ap} *vs.* [**L1**]. The binding constant, K = (slope/intercept) = 2.61 × 10^5 M^{-1}

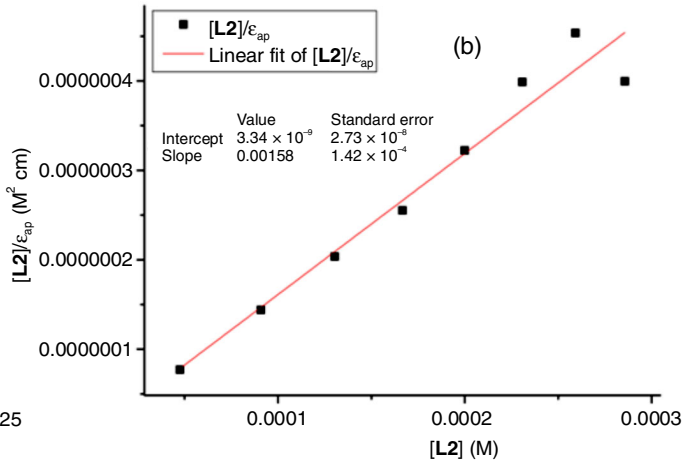

Fig. 5b. **L2**–Salicylic acid: plot of [**L2**]/ε_{ap} *vs.* [**L2**]. The binding constant, K = (slope/intercept) = 2.73 × 10^5 M^{-1}

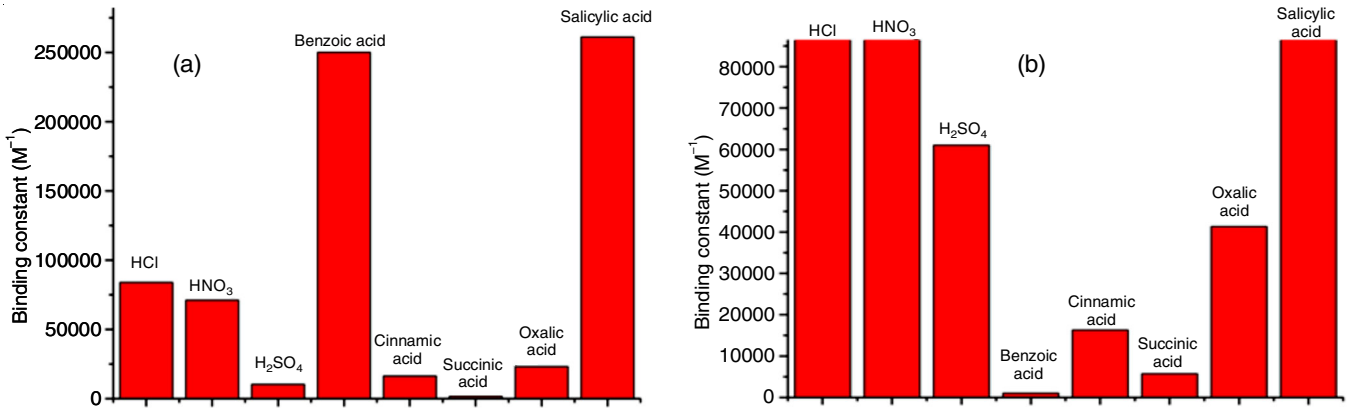

Fig. 6. Comparison of binding constants of different acids with compound **L1** (a) and **L2** (b)

binding affinity. This is also evident from the formation of isosbestic point with these acids (Fig. 3c-d). Hence, the protonated form of hosts **L1** and **L2** are potentially capable of distinguishing the anions obtained by deprotonation of the different types of acids.

Interaction of metal ions with L1 and L2 in solution state: Interaction of different metal ions with **L1** and **L2** were studied in solution state by conducting UV-visible titration experiment. A significant bathochromic shift in absorption maxima of **L2** on addition of Hg^{2+} ion was observed (Fig. 7a). On gradual addition of Hg^{2+} ion to a methanolic solution of **L2**, the absorption maximum was shifted from 377 nm to 401 nm with simultaneous formation of an isosbestic point at 298 nm. However, addition of Hg^{2+} ion to **L1** does not lead to any

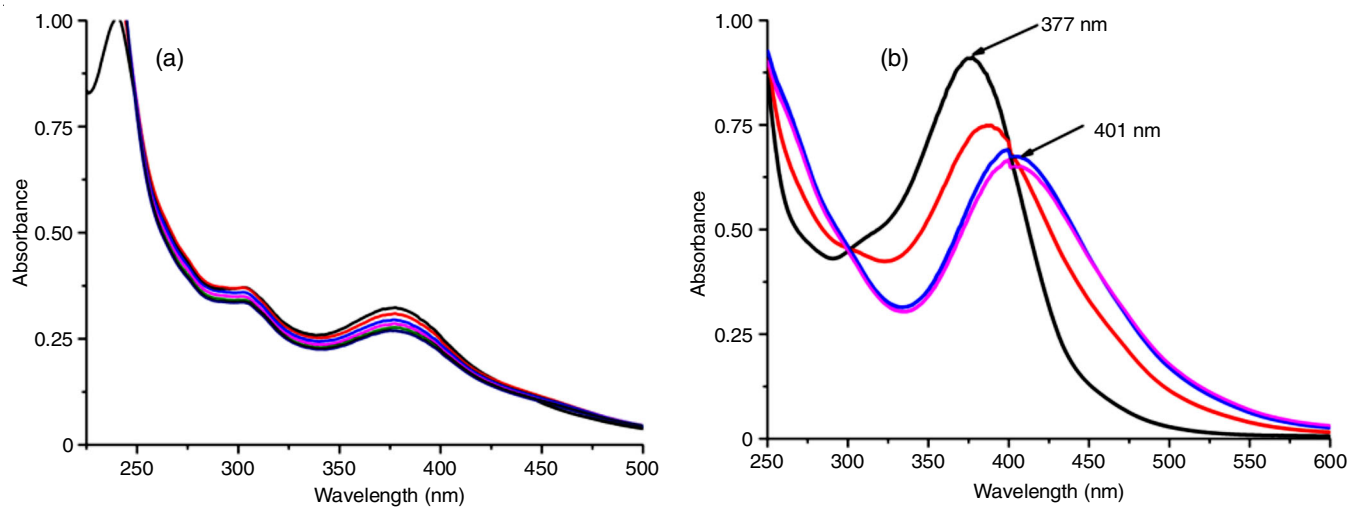

Fig. 7. UV-visible titration of **L1** (a) and **L2** (b) in the presence of increasing amounts of Hg^{2+} ion

significant change (Fig. 7b) showing the weak affinity for Hg^{2+} ion. This observation indicates that the presence of Hg^{2+} ion may be detected by using **L2** in solution state. The binding constant data also shows that the host **L2** has highest affinity towards Hg^{2+} ion in comparison to other metal ions (Fig. 9b).

After observing this attention-grabbing behaviour of Hg^{2+} ion towards the prepared receptors, we have extended this study with other metal ions such as Cu^{2+}, Fe^{2+}, Ni^{2+}, Zn^{2+}, Cd^{2+}, Mn^{2+} and Cr^{2+}. The receptor **L2** shows a considerable amount of bathochromic shift in the absorption maxima on addition of Cu^{2+} and Fe^{2+} ions to 391 nm and 385 nm, respectively (Fig. 8b). Whereas, with other metal ions such shifts in absorption maxima were not observed. Furthermore, receptor **L1** do not show such shift in absorption maxima with either of metal ions, instead it gives additional peak at 264 nm and 301 nm with Cu^{2+} and Fe^{2+} ions respectively (Fig. 8a).

The study of interaction of metal ions with **L1** and **L2** reveals its selective metal recognition properties. The binding constant values of **L1** and **L2** with different metal ions were calculated from UV-visible titration data. The affinity of these hosts towards different metal ions was studied by comparing their respective binding constant values. A comparative study of binding affinity of **L1** and **L2** is illustrated in Fig. 9a-b, respectively. Since **L2** is capable of detecting Hg^{2+} ion in solution state, we have also calculated the detection limit of Hg^{2+} ion in methanolic solution which is found to be 0.223 ppm. Hence, receptor **L2** will find application in detection of hazardous Hg^{2+} ion.

Theoretical interaction study of guest anions and metal ions with receptors L1 & L2: The optimized structures of two azo based receptors, **L1** and **L2** are shown in Fig. 10a-b, respectively. The Mulliken charge density of the nitrogen atoms (Table-1) indicates the possibility of protonation of N10 (**L1** & **L2**), N23 (**L2**), N27 & N28 (**L1**). It has been observed that the most stable protonation sites are N10 of **L1** and N23 of **L2**. However, the N10 atom of **L1** will experience a considerable amount of steric hindrance due to the intramolecular hydrogen bonding between N17-H19 and N10 which also persist after the formation of acid complexes (Fig. 10). Further investigations, therefore, were performed by considering protonation of N27 of **L1** and N23 of **L2**.

The binding constants of different acids with **L2** were calculated from the free energy change data and it is found to be in good agreement with experimental values. The unusual

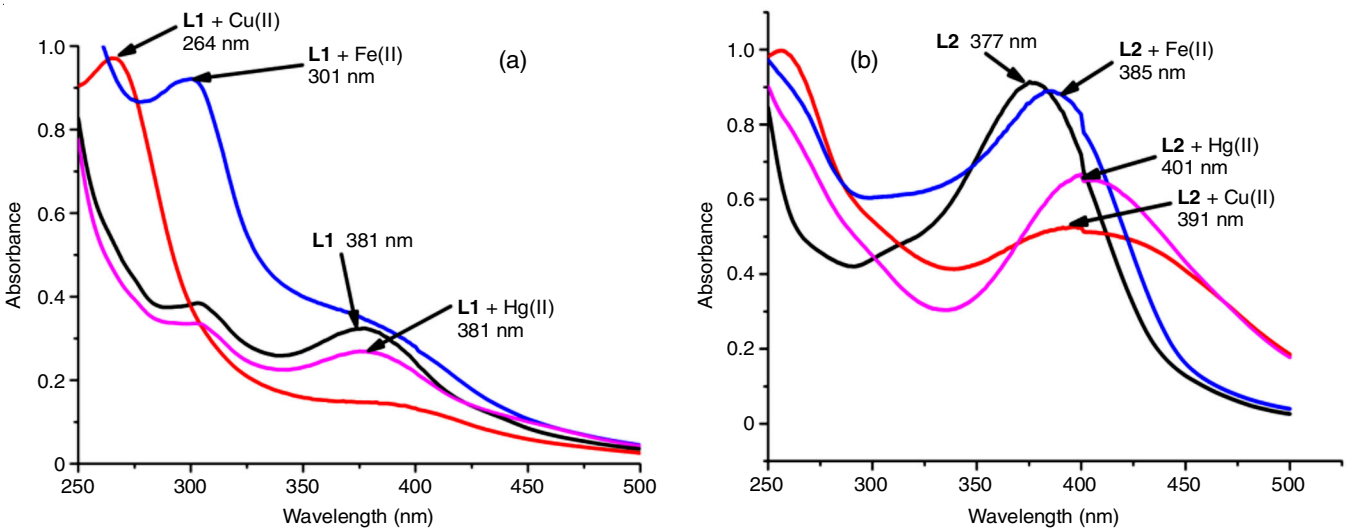

Fig. 8. Comparison of UV-visible spectra of **L1** ([**L1**] = 1×10^{-4} M in methanol) and **L1** + metal ions (1×10^{-4} M in methanol) (a) and **L2** ([**L2**] = 1×10^{-4} M in methanol) and **L2** + metal ions (1×10^{-4} M in methanol) (b)

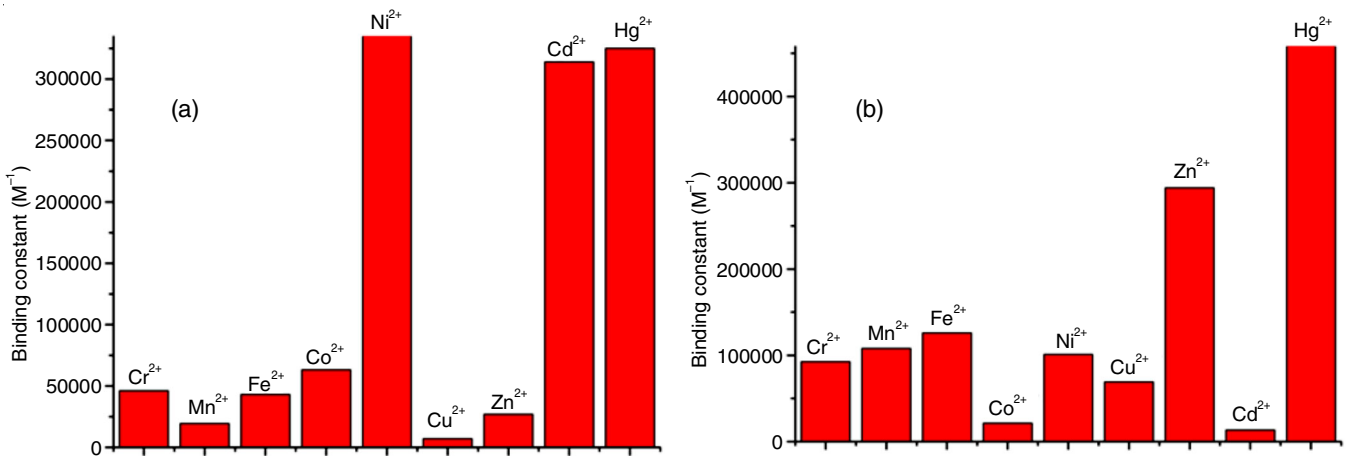

Fig. 9. Comparison of binding constants of different metal ions with **L1** (a) and **L2** (b)

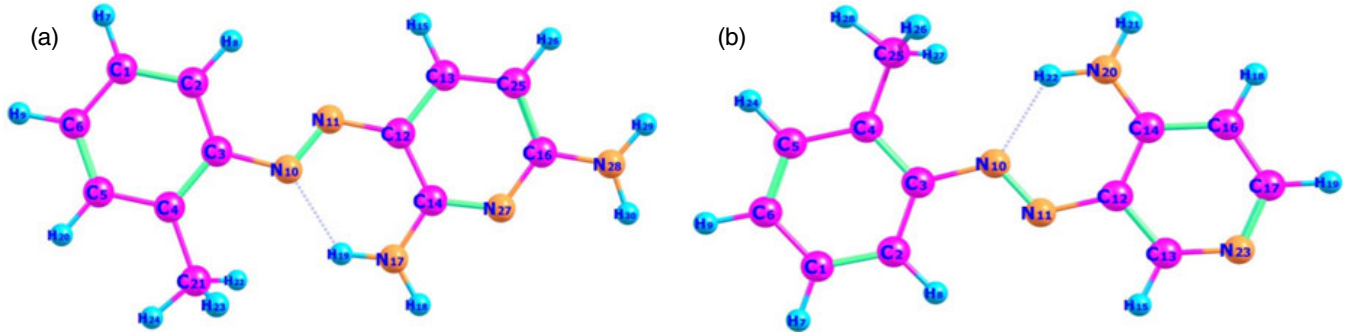

Fig. 10. Optimized structure of **L1** (a) and **L2** (b)

TABLE-1
MULLIKEN CHARGE DENSITIES AND STABILIZATION ENERGIES (kcal/mol)
ON PROTONATION OF NITROGEN ATOMS OF THE TWO COMPOUNDS

	Atom	N10	N11	N17	N27	N28
L1	Mulliken charge density	-0.2086	-0.0678	-0.0590	-0.1897	-0.1095
	Stabilization energies	-237.3992	-235.0204	-237.3992	-236.7880	-218.3830
	Atom	N10	N11	N20	N23	–
L2	Mulliken charge density	-0.1881	-0.0789	-0.0699	-0.1635	–
	Stabilization energies	-222.1525	-225.0596	-222.1525	-245.0782	–

affinity of Hg^{2+} ion towards **L2** observed in UV-visible study prompted us to perform further theoretical investigation of metal interaction with **L1** and **L2**. Hence, a similar study was also performed to investigate the binding effect of metals ions, Fe^{2+}, Cu^{2+} and Hg^{2+} with **L1** and **L2** (Table-2). Among the metals, Hg^{2+} ion shows higher stability with **L1** and **L2**. Among the receptors **L1** and **L2**; **L2** interact more efficiently with Hg^{2+} ion (Fig. 11a). The investigation leads to the plausibility of chloride coordinated copper complex of **L1** unlike to the stable octahedral aqua-coordinated geometry of other metal-ligand complexes (Fig. 11b).

HOMO–LUMO energies are the indicator of chemical reactivity of the reacting species. Higher HOMO energy signifies the greater ability to donate electrons and lower LUMO energy signifies greater ability to accept electrons [38,39]. The closeness of HOMO energy values for **L1** and **L2** complex with the three metal ions indicate the similar electron donating ability of the ligands (Table-2). Moreover, the negative HOMO energies are an indicator of stable metal complexes of the ligands [40]. The energy gap ΔE for **L1** with Hg^{2+} is small (90.1780 kcal/mol), which implies the reasonably higher reactivity of Hg^{2+} ion toward **L1**. However, in case of **L2**, both Cu^{2+} and Hg^{2+} have significant reactivity as indicated by the lower calculated energy gaps (102.5272 & 114.2615 kcal/mol). But the stability of **L2**-Hg^{2+} was found to be more than **L2**-Cu^{2+} and **L1**-Hg^{2+}.

TABLE-2
STABILIZATION ENERGY, HOMO-LUMO ENERGIES AND ENERGY GAP (kcal/mol) OF METAL COMPLEXES

Metal	**L1**				**L2**			
	Stability	E_{HOMO}	E_{LUMO}	ΔE	Stability	E_{HOMO}	E_{LUMO}	ΔE
Fe^{2+}	-26.3545	-282.9837	-156.3730	126.6107	-35.3104	-280.5615	-153.9446	126.6170
Cu^{2+}	-10.2562	-164.1226	-36.3009	127.7904	-37.2939	-280.3105	-152.1437	102.5272
Hg^{2+}	-35.4683	-261.9185	-171.7405	90.1780	-41.4663	-282.5507	-168.2892	114.2615

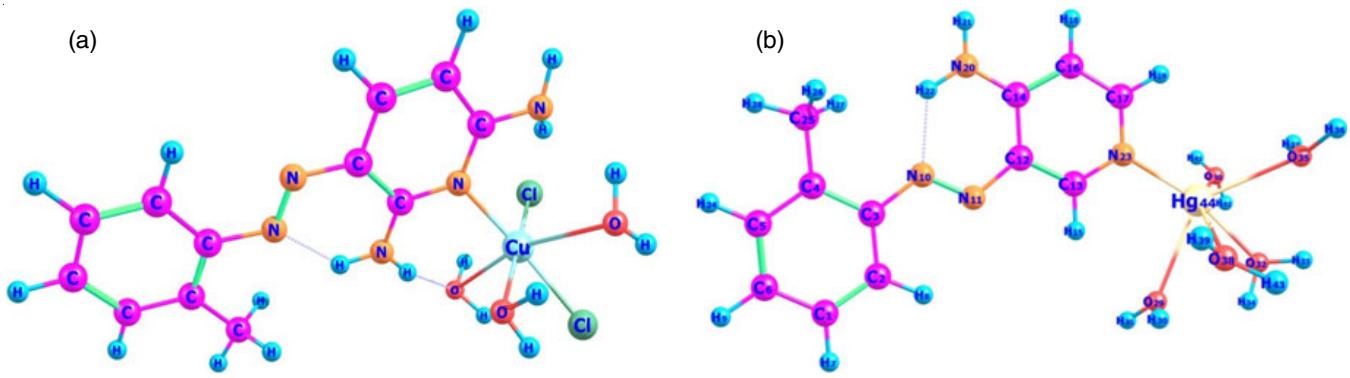

Fig. 11. Optimized structure of **L1**-Cu^{2+} complex (a) and **L2**-Hg^{2+} complex (b)

The HOMO-LUMO plot of **L1**-Hg^{2+} and **L2**-Hg^{2+} complexes are shown in Fig. 12. In both cases, the HOMO is ligand centric and the LUMO is metal centric whereas, similar HOMO-LUMO plots of copper and iron metal complexes does not show any metal centric LUMO.

The bond lengths of different complexes as well as molecules and the ions are also analyzed. It has been found that there is strong intramolecular hydrogen bonding between amine group hydrogen and the diazo nitrogen (N10) before and after complex formation. As a result, there is a strong steric hindrance that will be experienced by the guest molecules to get closure through this site. The shortest hydrogen bond (1.7770 Å) between N10-H19 of **L1** was found for **L1**-Fe^{2+} complex. However, for **L2** the lengths of N10-H22 hydrogen bonds are nearly same and close to 1.9492 Å, the hydrogen bond length in **L2** molecule. The N10-N11 bond lengths of **L1** and **L2** do not change significantly even after complex formation. It signifies the less possibility of complex formation with N10 or N11 of **L1** and **L2**. The change of C14-N27, C16-N27 bond length of **L1** and C17-N23, C13-N23 bond length of **L2** with respect to the free molecules were due to the formation of complex with acids and metal. The changes are more significant for metals, which indicate high metal affinity of the both the molecules.

The structures of different host-guest complexes of **L1** and **L2** were optimized and studied (Fig. 13a-b). A complete proton transfers from the acid to the N27 of **L1** was observed in case of nitric acid and sulphuric acid complexes, which is in agreement with their strong acidic behaviour of the guest

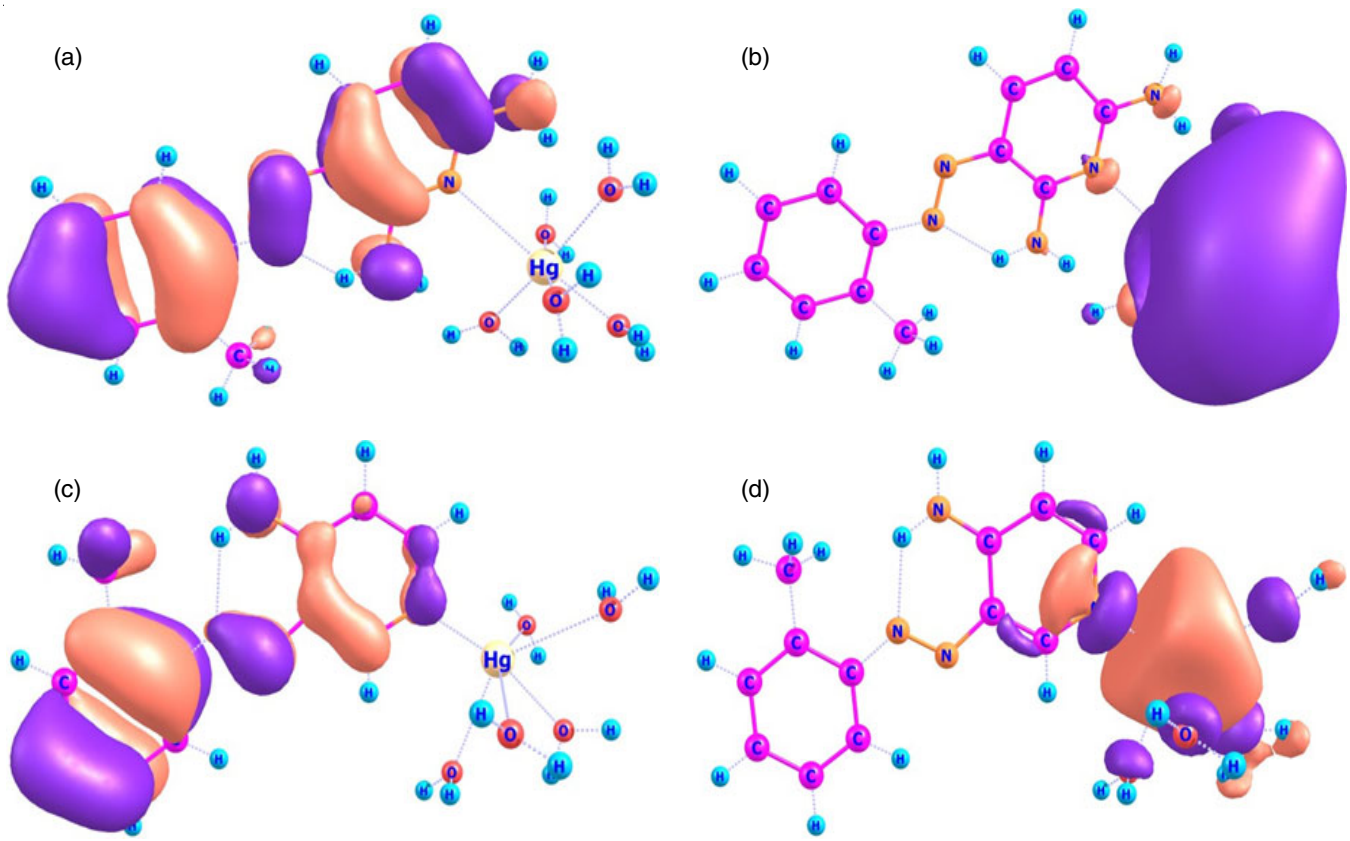

Fig. 12. Three dimensional HOMO and LUMO of **L1**-Hg^{2+} complex (a-b) and **L2**-Hg^{2+} complex (c-d)

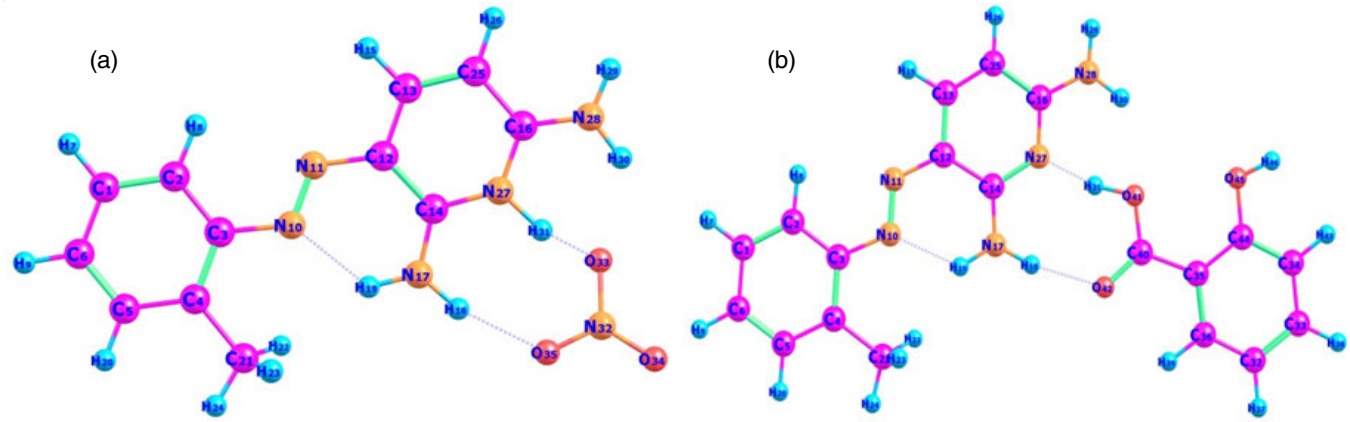

Fig. 13. Optimized structure of **L1** with nitric acid (a) and **L1** with salicylic acid (b)

molecules. The bond lengths of acid O-H for nitric acid (H31-O33) and sulphuric acid (H31-O35) after and before complex formation also indicate the protonation of **L1** by the two acids. However, with organic acid such as benzoic acid, cinnamic acid, salicylic acid, protonation of the receptor was not observed. In contrast, receptor **L2** do not show protonation with any of the acid.

Conclusion

Two supramolecular receptors (**L1** and **L2**) capable of binding anion as well as metal ion were synthesized. The interaction of the prepared hosts with different acids and metal ions were studied in solution state by using UV-visible titration experiment. The host **L1** binds almost all acids except benzoic acid whereas host **L2** shows the highest affinity to bind benzoic acid. The binding affinities were studied from their respective binding constants calculated from UV-visible titration experiment. A similar study with metal ions revealed that host **L2** shows a significant bathochromic shift in absorption maxima on interaction with Hg^{2+} ion and also highest affinity towards Hg^{2+} ion of **L2** was established from binding constant data. The receptor is capable of detecting Hg^{2+} ion in solution upto 0.223 ppm. To support this finding, theoretical calculations with these receptors with different host acids and metal ions are also done. Theoretical studies also suggest that these receptors are capable of binding strongly Hg^{2+} ions. Thus, supramolecular receptors **L1** and **L2** are capable of detecting anions and metal ions in solution state.

ACKNOWLEDGEMENTS

The authors are grateful to Department of Chemistry, Bhattadev University, Assam, India; HRMS facility, CIF Gauhati University, Assam, India for instrumentation facility; and Dr. Ankur Guha, Assistant Professor, Cotton University.

CONFLICT OF INTEREST

The authors declare that there is no conflict of interests regarding the publication of this article.

REFERENCES

1. J. Jansen, K. Jansen, E. Neven, R. Poesen, A. Othman, J.S. Torano, A. van Mil, J. Sluijter, C.R. Berkers, D. Esser, H.J. Wichers, K. van Ede, E.A. Zaal, M. van Duursen, S. Burtey, M.C. Verhaar, B. Meijers and R. Masereeuw, *Proc. Natl. Acad. Sci. USA*, **116**, 16105 (2019); https://doi.org/10.1073/pnas.1821809116
2. J. Pancholi and P.D. Beer, *Coord. Chem. Rev.*, **416**, 213281 (2020); https://doi.org/10.1016/j.ccr.2020.213281
3. T.J. Costa, P.R. Barros, C. Arce, J.D. Santos, J. da Silva-Neto, G. Egea, A.P. Dantas, R.C. Tostes and F. Jimenez-Altayo, *Free Radic. Biol. Med.*, **162**, 615 (2021); https://doi.org/10.1016/j.freeradbiomed.2020.11.021
4. C. Cendra, A. Giovannitti, A. Savva, V. Venkatraman, I. McCulloch, A. Salleo, S. Inal and J. Rivnay, *Adv. Funct. Mater.*, **29**, 1807034 (2019); https://doi.org/10.1002/adfm.201807034
5. Z. Huang, T. Wang, H. Song, X. Li, G. Liang, D. Wang, Q. Yang, Z. Chen, L. Ma, Z. Liu, B. Gao, J. Fan and C. Zhi, *Angew. Chem.*, **133**, 1024 (2021); https://doi.org/10.1002/ange.202012202
6. R. Steudel and T. Chivers, *Chem. Soc. Rev.*, **48**, 3279 (2019); https://doi.org/10.1039/C8CS00826D
7. D. Yuan, J. Zhao, H. Ren, Y. Chen, R. Chua, E.T.J. Jie, Y. Cai, E. Edison, W. Manalastas Jr., M.W. Wong and M. Srinivasan, *Angew. Chem.*, **133**, 7289 (2021); https://doi.org/10.1002/ange.202015488
8. J.F. Ding, R. Xu, N. Yao, X. Chen, Y. Xiao, Y.-X. Yao, C. Yan, J. Xie and J.-Q. Huang, *Angew. Chem. Int. Ed.*, **60**, 11442 (2021); https://doi.org/10.1002/anie.202101627
9. E. Muszyñska and M. Labudda, *Int. J. Mol. Sci.*, **20**, 3117 (2019); https://doi.org/10.3390/ijms20133117
10. H. Sies, V.V. Belousov, N.S. Chandel, M.J. Davies, D.P. Jones, G.E. Mann, M.P. Murphy, M. Yamamoto and C. Winterbourn, *Nat. Rev. Mol. Cell Biol.*, **23**, 499 (2022); https://doi.org/10.1038/s41580-022-00456-z
11. V. Juvekar, S.J. Park, J. Yoon and H.M. Kim, *Coord. Chem. Rev.*, **427**, 213574 (2021); https://doi.org/10.1016/j.ccr.2020.213574
12. S. Elçin, M.M. Ilhan and H. Deligöz, *J. Incl. Phenom. Macrocycl. Chem.*, **77**, 259 (2013); https://doi.org/10.1007/s10847-012-0240-7
13. A. Panitsiri, S. Tongkhan, W. Radchatawedchakoon and U. Sakee, *J. Mol. Struct.*, **1107**, 14 (2016); https://doi.org/10.1016/j.molstruc.2015.11.013
14. M.R. Maliyappa, J. Keshavayya, M. Mahanthappa, Y. Shivaraj and K.V. Basavarajappa, *J. Mol. Struct.*, **1199**, 126959 (2020); https://doi.org/10.1016/j.molstruc.2019.126959
15. F. Qiu, C. Chen, Q. Zhou, Z. Cao, G. Cao, Y. Guan and D. Yang, *Opt. Mater.*, **36**, 1153 (2014); https://doi.org/10.1016/j.optmat.2014.02.019
16. D. Li, Y. Luo, D. Onidas, L. He, M. Jin, F. Gazeau, J. Pinson and C. Mangeney, *Adv. Colloid Interface Sci.*, **294**, 102479 (2021); https://doi.org/10.1016/j.cis.2021.102479
17. S. Prakash, G. Somiya, N. Elavarasan, K. Subashini, R. Dhandapani, S. Kanaga, M. Sivanandam, P. Kumaradhas, C. Thirunavukkarasu and V. Sujatha, *J. Mol. Struct.*, **1224**, 129016 (2021); https://doi.org/10.1016/j.molstruc.2020.129016
18. F.T. Souto, J.L. de O. Buske, C.R. Nicoleti, J.P. Dreyer, R. da S. Heying, A.J. Bortoluzzi and V.G. Machado, *Spectrochim. Acta A Mol. Biomol. Spectrosc.*, **260**, 119950 (2021); https://doi.org/10.1016/j.saa.2021.119950
19. S. Kamali, M. Orojloo, R. Arabahmadi and S. Amani, *J. Photochem. Photobiol. Chem.*, **433**, 114136 (2022); https://doi.org/10.1016/j.jphotochem.2022.114136
20. M.N. ElNahass, T.A. Fayed, H.A. ElDaly and M.M. Youssif, *Appl. Organomet. Chem.*, **36**, e6703 (2022); https://doi.org/10.1002/aoc.6703
21. N. Chakraborty, A. Chakraborty and S. Das, *J. Heterocycl. Chem.*, **56**, 2993 (2019); https://doi.org/10.1002/jhet.3693
22. G.W. Lee, N.-K. Kim and K.-S. Jeong, *Org. Lett.*, **12**, 2634 (2010); https://doi.org/10.1021/ol100830b
23. T.S. Basu Baul, A. Mizar, A. Paul, G. Ruisi, R. Willem, M. Biesemans and A. Linden, *J. Organomet. Chem.*, **694**, 2142 (2009); https://doi.org/10.1016/j.jorganchem.2009.02.021
24. M. Pervaiz, S. Sadiq, A. Sadiq, U. Younas, A. Ashraf, Z. Saeed, M. Zuber and A. Adnan, *Coord. Chem. Rev.*, **447**, 214128 (2021); https://doi.org/10.1016/j.ccr.2021.214128
25. R. Gup, E. Giziroglu and B. Kirkan, *Dyes Pigments*, **73**, 40 (2007); https://doi.org/10.1016/j.dyepig.2005.10.005
26. J. Durka, J. Turkowska and D. Gryko, *ACS Sustain. Chem. Eng.*, **9**, 8895 (2021); https://doi.org/10.1021/acssuschemeng.1c01976
27. G.R. Ferreira, B.L. Marcial, H.C. Garcia, F.R.L. Faulstich, H.F. Dos Santos and L.F.C. de Oliveira, *Supramol. Chem.*, **27**, 13 (2015); https://doi.org/10.1080/10610278.2014.899598
28. M. Yahya, N. Seferoglu, G. Kaplan, Y. Nural, A. Barsella and Z. Seferoglu, *J. Mol. Struct.*, **1273**, 134257 (2023); https://doi.org/10.1016/j.molstruc.2022.134257
29. A.A. Balakit, S.Q. Makki, Y. Sert, F. Ucun, M.B. Alshammari, P. Thordarson and G.A. El-Hiti, *Supramol. Chem.*, **32**, 519 (2020); https://doi.org/10.1080/10610278.2020.1808217

30. J.R. Penton and H. Zollinger, *Helv. Chim. Acta*, **64**, 1728 (1981); https://doi.org/10.1002/hlca.19810640603
31. R.N. Shreve, M.W. Swaney and E.H. Riechers, *J. Am. Chem. Soc.*, **65**, 2241 (1943); https://doi.org/10.1021/ja01251a066
32. S. Priya Bharati, B. Chandra Mushahary, R. Das and S.P. Mahanta, *Results Chem.*, **5**, 100927 (2023); https://doi.org/10.1016/j.rechem.2023.100927
33. M.J. Frisch, G.W. Trucks, H.B. Schlegel, G.E. Scuseria, M.A. Robb, J. R. Cheeseman, G. Scalmani, V. Barone, G. A. Petersson, H. Nakatsuji, X. Li, M. Caricato, A.V. Marenich, J. Bloino, B.G. Janesko, R. Gomperts, B. Mennucci, H.P. Hratchian, J.V. Ortiz, A.F. Izmaylov, J.L. Sonnenberg, D. Williams-Young, F. Ding, F. Lipparini, F. Egidi, J. Goings, B. Peng, A. Petrone, T. Henderson, D. Ranasinghe, V.G. Zakrzewski, J. Gao, N. Rega, G. Zheng, W. Liang, M. Hada, M. Ehara, K. Toyota, R. Fukuda, J. Hasegawa, M. Ishida, T. Nakajima, Y. Honda, O. Kitao, H. Nakai, T. Vreven, K. Throssell, J.A. Montgomery Jr., J.E. Peralta, F. Ogliaro, M.J. Bearpark, J.J. Heyd, E.N. Brothers, K.N. Kudin, V.N. Staroverov, T.A. Keith, R. Kobayashi, J. Normand, K. Raghavachari, A.P. Rendell, J.C. Burant, S.S. Iyengar, J. Tomasi, M. Cossi, J.M. Millam, M. Klene, C. Adamo, R. Cammi, J.W. Ochterski, R.L. Martin, K. Morokuma, O. Farkas, J.B. Foresman and D.J. Fox, Gaussian, Inc., Wallingford CT, 2016.
34. Y. Zhao and D.G. Truhlar, *Theor. Chem. Acc.*, **120**, 215 (2008); https://doi.org/10.1007/s00214-007-0310-x
35. M.B. Robin and W.T. Simpson, *J. Chem. Phys.*, **36**, 580 (1962); https://doi.org/10.1063/1.1732574
36. H. Rau, *Angew. Chem. Int. Ed. Engl.*, **12**, 224 (1973); https://doi.org/10.1002/anie.197302241
37. A.D. Tiwari, A.K. Mishra, S.B. Mishra, B.B. Mamba, S. Bhattacharya and B. Maji, *Spectrochim. Acta A Mol. Biomol. Spectrosc.*, **79**, 1050 (2011); https://doi.org/10.1016/j.saa.2011.04.018
38. K. Fukui, *Science*, **218**, 747 (1982); https://doi.org/10.1126/science.218.4574.747
39. G. Gao and C. Liang, *Electrochim. Acta*, **52**, 4554 (2007); https://doi.org/10.1016/j.electacta.2006.12.058
40. H.A. ElGhamry, S.K. Fathalla and M. Gaber, *Appl. Organomet. Chem.*, **32**, e4136 (2018); https://doi.org/10.1002/aoc.4136